Finite-temperature entanglement and coherence in asymmetric bosonic Josephson junctions

Luca Salasnich*

in collaboration with

M. Ferraretto and C. Vianello

*Dipartimento di Fisica e Astronomia "Galileo Galilei", Università di Padova, and INFN, Sezione di Padova

FisMat2025, Venice, July 8, 2025

Summary

- Two-site Bose-Hubbard model
- Semiclassical approximation
- Exact diagonalization: Thermal equilibrium
- Exact diagonalization: Entanglement entropy
- Coherence visibility: Exact vs semiclassical
- Conclusions

Two-site Bose-Hubbard model

A system of N interacting bosons confined by an asymmetric double-well potential can be described by the two-site Bose-Hubbard model[1]

$$\hat{H} = -J(\hat{a}_L^\dagger \hat{a}_R + \hat{a}_R^\dagger \hat{a}_L) + \frac{U}{2}[\hat{N}_L(\hat{N}_L - 1) + \hat{N}_R(\hat{N}_R - 1)] + \frac{\varepsilon}{2}(\hat{N}_L - \hat{N}_R) \quad (1)$$

with $J > 0$ the tunneling (hopping) energy, U the boson-boson interaction, and ε the on-site energy asymmetry.

Semiclassical (mean-field) dynamics.

Taking the expectation value of the Heisenberg equations on **Glauber coherent states**, after defining $\langle \hat{a}_j(t) \rangle = \sqrt{N_j(t)}\, e^{i\theta_j(t)}$ one obtains[2]

$$\hbar\dot{\theta}(t) = \frac{2J\,z(t)}{\sqrt{1 - z(t)^2}} \cos(\theta(t)) + UN\,z(t) + \varepsilon, \quad (2)$$

$$\hbar\dot{z}(t) = -2J\sqrt{1 - z(t)^2}\,\sin(\theta(t)) \quad (3)$$

where $\theta(t) = \theta_R(t) - \theta_L(t)$ is the relative phase and $z(t) = (N_L(t) - N_R(t))/N$ is the population imbalance. Here $N = N_L(t) + N_R(t)$ and $\langle \hat{N}_j(t) \rangle = N_j(t)$.

---

[1] M. Lewenstein, A. Sanpera, V. Ahufinger, Ultracold atoms in optical lattice (Oxford Univ, Press 2012).

[2] A Smerzi, S Fantoni, S Giovanazzi, SR Shenoy Phys. Rev. Lett. **79**, 4950 (1997).

Semiclassical approximation

Introducing the canonical momentum

$$p_\theta(t) = \frac{\hbar N}{2} z(t) \tag{4}$$

the equations of motion of the first slide can be regarded as the canonical Hamilton equations for

$$H = \frac{U}{\hbar^2} p_\theta^2 + \frac{\varepsilon}{\hbar} p_\theta - JN \sqrt{1 - \frac{4}{\hbar^2 N^2} p_\theta^2} \cos(\theta) \tag{5}$$

For $|U|/J \gg 1/N$, we get the **semiclasical** Josephson Hamiltonian[3]

$$H_J = \frac{U}{\hbar^2} p_\theta^2 + \frac{\varepsilon}{\hbar} p_\theta - JN \cos(\theta) \tag{6}$$

that is the key ingredient for our semiclassical analysis both at zero and finite temperature T.

[3] K. Furutani, J. Tempere, LS, Phys. Rev. B **105**, 134510 (2022).

Semiclassical approximation

For $1/N \ll U/J \ll N$, the semiclassical dynamics of H_J describes small oscillations around $z = 0$ and $\theta = 0$ with Josephson frequency

$$\omega_J = \frac{\sqrt{2UJN}}{\hbar} \; . \tag{7}$$

At low energies the distribution of quantum-thermal states is essentially that of an harmonic oscillator with Josephson frequency ω_J, which differs from the Boltzmann distribution by the fact that the temperature T of the bath is replaced by[4]

$$T_{\rm eff} = \frac{\hbar\omega_J}{2k_B} \coth\left(\frac{\hbar\omega_J}{2k_B T}\right) . \tag{8}$$

This provides us with a **semiclassical approximation** for the thermal averages of observables:

$$\langle \hat{O} \rangle = \frac{1}{\mathcal{Z}} \int_{-\hbar N/2}^{\hbar N/2} dp_\theta \int_{-\pi}^{\pi} d\theta \, O(p_\theta, \theta) \, e^{-H_J(p_\theta,\theta)/(k_B T_{\rm eff})} \tag{9}$$

[4] K. Furutani and LS, AAPPS Bull. **33**, 19 (2023).

Exact diagonalization: Thermal equilibrium

At fixed N, the diagonalization[5] of the $(N+1)\times(N+1)$ matrix associated to the Hamiltonian $\hat{H}$ gives $N+1$ eigenvalues E_n and $N+1$ eigenstates $|E_n\rangle$.
At thermal equilibrium with a bath of temperature T the density matrix reads

$$\hat{\rho} = \frac{1}{\mathcal{Z}} \sum_{n=0}^{N} e^{-E_n/(k_B T)} |\, E_n \,\rangle\langle\, E_n \,| = \sum_{i,j=0}^{N} \rho_{ij} |\, i, N-i \,\rangle\langle j, N-j \,| \qquad (10)$$

where $|\, E_n \,\rangle = \sum_{i=0}^{N} c_i^{(n)} |\, i, N-i \,\rangle$ with $|i, N-i\rangle = |i\rangle_L |N-i\rangle_R$, and

$$\rho_{ij} = \frac{1}{\mathcal{Z}} \sum_{n=0}^{N} e^{-E_n/(k_B T)} c_i^{(n)} (c_j^{(n)})^* \qquad (11)$$

The diagonal elements $\rho_{ii} = \langle |c_i|^2 \rangle = \sum_{n=0}^{N} |c_i^{(n)}|^2 e^{-E_n/(k_B T)}/\mathcal{Z}$ represent the average weights of the Fock states $|\, i, N-i \,\rangle$ in the statistical ensemble.
Thermal averages are computed as

$$\langle \hat{O} \rangle = \mathrm{Tr}[\hat{\rho}\, \hat{O}] = \sum_{i,j=0}^{N} \rho_{ij} \langle\, i, N-i \,|\, \hat{O} \,|\, j, N-j \,\rangle \qquad (12)$$

[5] G. Mazzarella, LS, A. Parola, F. Toigo, Phys. Rev. A **83**, 053607 (2011).

Exact diagonalization: Thermal equilibrium

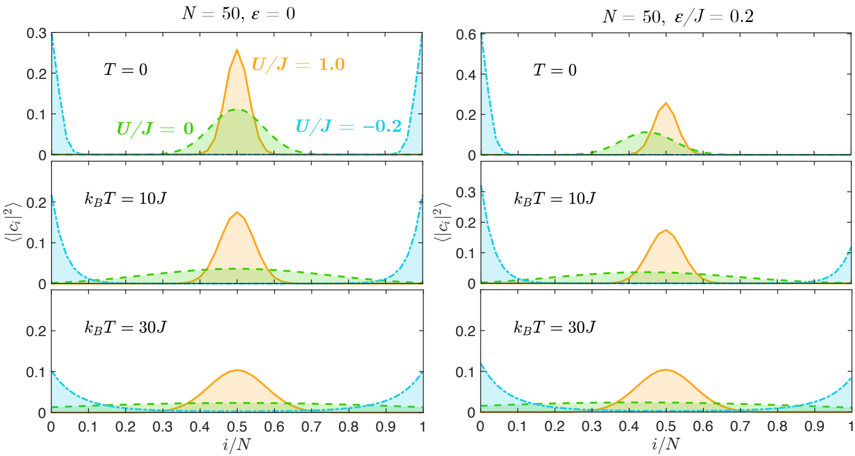

Thermal average $\rho_{ii} = \langle |c_i|^2 \rangle$ **of Fock weights** as a function of i/N , plotted for N $= 50$ and three values of U/J: 1 (solid orange line), 0 (dashed green line), -0.2 (dashed-dotted cyan line) at different temperatures T. **Left**: $\varepsilon/J = 0$; **right**: $\varepsilon/J = 0.2$.

Exact diagonalization: Entanglement entropy

The **entanglement** between the two wells can be characterized[6] in terms of the reduced density matrices $\hat{\rho}_{L(R)} = \mathrm{Tr}_{R(L)}[\hat{\rho}]$,

$$\hat{\rho}_L = \hat{\rho}_R = \sum_{n=0}^{N} \rho_n \, \hat{\rho}^{(n)}_{\mathrm{diag}} \tag{13}$$

where $\rho_n = e^{-E_n/(k_B T)}/\mathcal{Z}$ and

$$\hat{\rho}^{(n)}_{\mathrm{diag}} = \sum_{i=0}^{N} |c_i^{(n)}|^2 |\, i, N-i\,\rangle\langle\, i, N-i\,|. \tag{14}$$

The **entanglement entropy** $S_E = S_{\mathrm{vN}}[\hat{\rho}_L] = S_{\mathrm{v}N}[\hat{\rho}_R]$ is given by

$$S_E = -\sum_{i=0}^{N} \langle |c_i|^2 \rangle \, \ln\left(\langle |c_i|^2 \rangle\right) \qquad \in [0, \ln(N+1)] \tag{15}$$

that is the von Neumann entropy S_{vN} of the reduced density matrix $\hat{\rho}_L$, and also of $\hat{\rho}_R$.

[6] M. Le Bellac, A Short Introduction to Quantum Information and Quantum Computation (Cambridge Univ. Press, 2006).

Exact diagonalization: Entanglement entropy

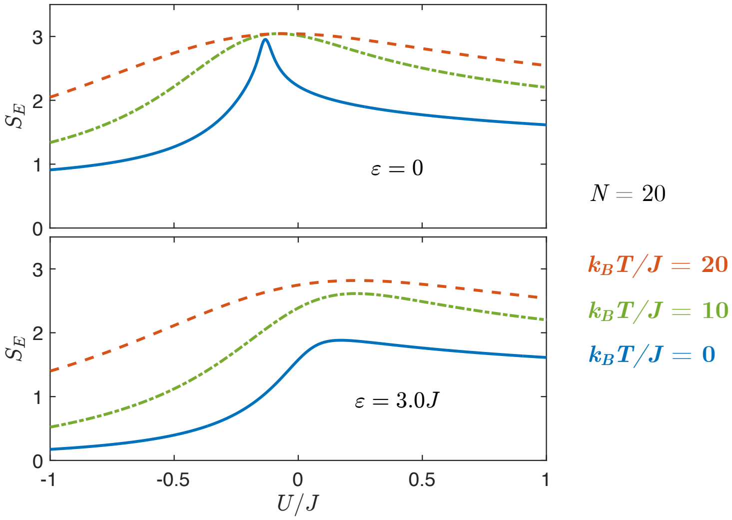

Entanglement entropy S_E as a function of U/J, plotted for $N = 20$ and three values of $k_B T/J$: 0 (solid blue line), 10 (dashed-dotted green line), 20 (dashed orange line). **Upper panel**: $\varepsilon/J = 0$; **lower panel**: $\varepsilon/J = 3$.

Coherence visibility: Exact vs semiclassical

The coherence of our system can be characterized in terms of the quantity

$$\alpha = \frac{2\langle \hat{a}_L^\dagger \hat{a}_R \rangle}{N} \tag{16}$$

called **coherence visibility**.[7] This is related to the occupation of the single-particle ground state (**condensate fraction**) by

$$\frac{\langle \hat{a}_0^\dagger \hat{a}_0 \rangle}{N} = \frac{1+\alpha}{2} \tag{17}$$

where $\hat{a}_0 = (\hat{a}_L + \hat{a}_R)/\sqrt{2}$ and $\hat{a}_1 = (\hat{a}_L - \hat{a}_R)/\sqrt{2}$.

Semiclassical method
By using the semiclassical approach, we get the quite simple formula

$$\alpha = \langle cos(\theta) \rangle = \frac{I_1(JN/(k_B T_{\rm eff}))}{I_0(JN/(k_B T_{\rm eff}))} \tag{18}$$

where $I_n(x)$ is the n-th modified Bessel function of the first kind.

[7] L. Pitaevskii and S. Stringari, Phys. Rev. Lett. **87**, 180402 (2001).

Coherence visibility: Exact vs semiclassical

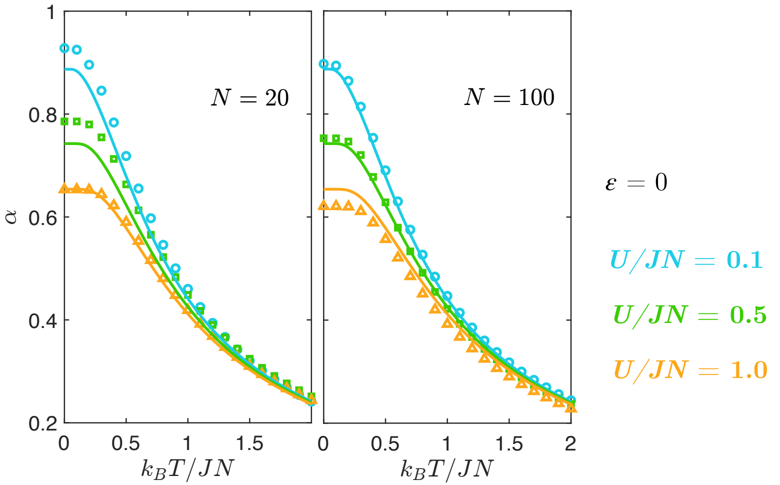

Coherence visibility α for $\varepsilon = 0$ as a function of $k_B T/JN$, plotted for $N = 20$ (**left panel**) and $N = 100$ (**right panel**), and three values of U/JN: 0.1 (cyan circles), 0.5 (green squares), 1 (orange triangles). The continuous lines are the corresponding semiclassical result.

Coherence visibility: Exact vs semiclassical

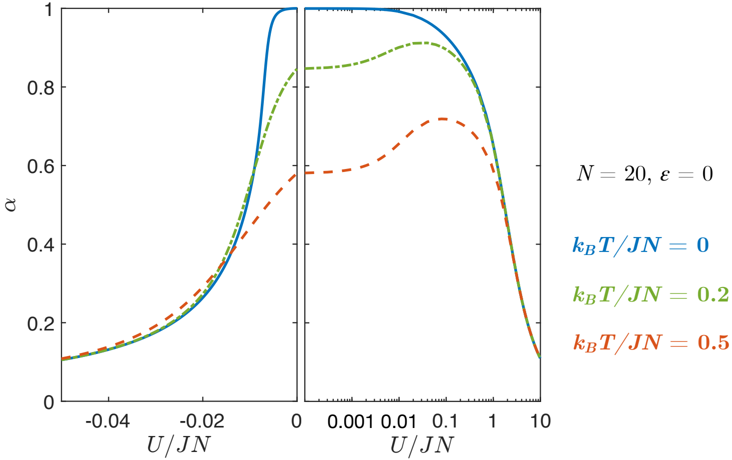

Coherence visibility α for $\varepsilon = 0$ as a function of U/JN, plotted for $N = 20$ and three values of $k_B T/JN$: 0 (solid blue line), 0.2 (dashed-dotted green line), 0.5 (dashed orange line).

Coherence visibility: Exact vs semiclassical

Introducing a small nonzero asymmetry energy ε, the coherence visibility α at $U = 0$ is significantly reduced both at zero and finite temperature T, while it remains almost unaffected for $|U|/JN > 0$.

In the repulsive regime the visibility α becomes a non-monotonic function of the interaction strength U at all temperatures (including $T = 0$), showing an initial increase before decreasing asymptotically to zero.

In the attractive regime the visibility α remains a monotonically decreasing function of the modulus of the interaction strength.

Conclusions

- We have characterized the thermal state of a bosonic Josephson junction by means of complementary observables (**entanglement entropy** and **coherence visibility**), analyzing their dependence on the system parameters, showing how interparticle interaction, finite temperature, and on-site energy asymmetry affect their properties.
- We have presented a **semiclassical description** of the strong tunneling regime, where thermal averages may be computed analytically using a modified Boltzmann weight involving an effective temperature.
- The **semiclassical description** may be applied
  - to describe thermal properties of more complicated bosonic junctions (dipolar interactions, multi-component);
  - to investigate quantum dissipative systems.
- Our results are **published** in the paper:
  C. Vianello, M. Ferraretto, and LS, Phys. Rev. A **111**, 063310 (2025).

Thank you for your attention!